Remote Wigner polaron in a magnetic field

H. Kato* and F. M. Peeters†
University of Antwerp (UIA), Department of Physics, Universiteitsplein 1, B-2610 Antwerpen, Belgium
(Received 30 October 1998)

A remote electron moving a distance away and parallel to a two-dimensional electron system (2DES) in a perpendicular magnetic field is mapped into a polaron problem. In high magnetic fields the 2DES crystallizes into a Wigner lattice having two hybrid phonon modes which are neither longitudinal nor transverse. The remote electron interacts with these hybrid phonons and forms a composite quasiparticle of electron plus Wigner crystal distortion which is called a *Wigner polaron*. The ground-state energy of the Wigner polaron is calculated using second-order perturbation theory and the results are related to an experiment on resonant tunneling. [S0163-1829(99)00721-3]

I. INTRODUCTION

A two-dimensional electron system (2DES) can crystallize into a hexagonal crystal which is called a Wigner crystal (WC). At zero temperature this solid phase appears[1] when the electron density is less than $n_{\mathrm{c}}=4/\pi a_{\mathrm{B}}^2\Gamma^2$, where a_{B} $(=\hbar^2\epsilon/me^2)$ is the effective Bohr radius and $\Gamma(\simeq 137)$ is the plasma parameter. For a 2DES realized in a GaAs heterojunction this value n_{c} is about 6.9×10^7 cm^{-2}. For a 2DES in the classical regime, i.e., $E_{\mathrm{F}}<k_{\mathrm{B}}T$, this solid phase has been observed for electrons floating on liquid helium.[2,3] On the other hand, if a magnetic field is applied perpendicular to the system, the critical density increases due to the quenching of the kinetic energy of the electron. Andrei *et al.*[4] found experimentally that the 2DES crystallizes when the filling factor is less than a critical value $\nu_{\mathrm{c}}=0.23$ at very low temperature. This condition can be transformed into a critical electron density $n_{\mathrm{c}}=\nu_{\mathrm{c}}B/\phi_0$ where B is the magnetic field and ϕ_0 is the flux quantum. For a typical magnetic field of $B=20$ T this critical density is 1.1×10^{11} cm^{-2}. Consequently, the WC can exist in a large range of electron densities even in GaAs heterojunctions where the electron has a small effective mass and where usually the electron gas, in the absence of a magnetic field, behaves as a quantum gas.

A bilayer electron system (BLES) is realized in a high quality double-quantum well[5] or in a wide single-quantum well.[6] The distance between the two 2DES introduces a new degree of freedom through which the electron-electron interaction can be modified. For example, the quantum Hall effect is modified by the interlayer interaction[5,6] and different WC phases are predicted.[7] In the present paper we investigate the interaction of a single remote electron with a WC in the presence of an external magnetic field. In a previous paper we formulated the *Wigner polaron* in a BLES in the absence of a magnetic field.[8] The electron distorts the WC locally and the composite quasiparticle: electron + distortion is called the Wigner polaron. The resulting electron-phonon interaction in a BLES has the remarkable feature that its strength can be modified by changing the distance between the remote electron and the 2DES, giving rise to a continuous localization of the polaron for small bilayer separations.[8] Another difference with the traditional polaron problems is that the lattice distortion (or polarization) and the electron are spatially separated. An alternative experimental system is a double barrier tunneling structure[9] in which an electron tunnels in or out of a 2DES. When the 2DES is not in the crystal phase the electron will interact with the plasmon modes of the 2DES which results into the plasmon polaron which we discussed in Ref. 10.

A Wigner crystal has longitudinal and transverse phonon modes.[11,12] When a perpendicular magnetic field is applied, these two modes are coupled and new hybrid modes appear.[12,13] The Wigner polaron will be produced now by the polarization of these modes. In the present paper we will diagonalize the resulting phonon Hamiltonian and obtain the canonical coordinates using the Laplace transformation technique. After the evaluation of the polaron energy, including both static and dynamical mass-renormalization effects, we identify the obtained energy shifts with those observed in recent tunneling experiments.

The present paper is organized as follows. In Sec. II we discuss the mass modulation of a remote electron in the static periodic potential of a WC. In Sec. III the hybrid phonon modes induced by a magnetic-field are obtained and analyzed. In Sec. IV the distortion of the WC due to a remote electron is discussed in terms of a Wigner polaron. Polaron induced energy shifts are compared with the shift in the position of the tunnel current in a resonant tunneling device, and their magnetic-field dependence is analyzed. Finally, our conclusions are given in Sec. V.

II. ELECTRON BAND STRUCTURE INDUCED BY THE PERIODIC POTENTIAL OF A WIGNER CRYSTAL

In this section we consider the *static* WC and compute the influence of such a periodic potential on the energy spectrum of a remote electron. The potential energy of a remote electron a distance z separated from a WC lying in the xy plane is given by

$$\varphi(\mathbf{r},z)=\sum_{\mathbf{n}}\frac{e^2}{\epsilon\sqrt{(\mathbf{r}-\mathbf{R}_{\mathbf{n}})^2+z^2}}=\sum_{\mathbf{K}(\neq 0)}\varphi(\mathbf{K})\exp(-i\mathbf{K}\cdot\mathbf{r}), \tag{1}$$

where $\mathbf{r}$ is the 2D electron position, the lattice electrons are situated at the hexagonal sites $\mathbf{R}_{\mathbf{n}}$ with $\mathbf{n}$ the 2D lattice index, and the 2D Fourier transform of the periodic WC potential is

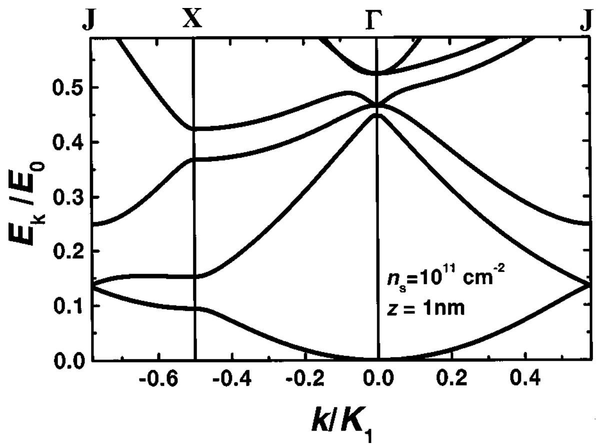

FIG. 1. The electron band structure caused by the periodic potential of the static WC. The remote electron is located at $z=1$ nm, the electron density of the 2DES is $n_s=10^{11}$ cm^{-2}, the unit of energy is $E_0=\hbar^2K_1^2/m=51.6$ meV, and the unit of wavelength is $K_1=4\pi/\sqrt{3}a=2.14\times10^6$ cm^{-1}, with a the WC lattice constant.

$$\varphi(\mathbf{K})=\frac{2\pi n_s}{\epsilon\Omega}\frac{\exp(-zK)}{K}, \tag{2}$$

where n_s is the electron density, ϵ the static dielectric constant of the medium the electrons are moving in, and Ω the 2D surface area. In this periodic potential the remote electron will be in a Bloch state and the wave function is given by

$$\psi(\mathbf{r})=\sum_{\mathbf{k}}\sum_{\mathbf{K}}F(\mathbf{K})\exp[i(\mathbf{K}+\mathbf{k})\cdot\mathbf{r}], \tag{3}$$

with $\mathbf{K}$ the 2D reciprocal-lattice vector. Then the Schrödinger equation for the remote electron in wave-vector space is given by

$$\left[\frac{\hbar^2}{2m}(\mathbf{k}+\mathbf{K})^2-E_{\mathbf{k}}\right]F(\mathbf{K})+\sum_{\mathbf{K}'}\varphi(\mathbf{K}-\mathbf{K}')F(\mathbf{K}')=0, \tag{4}$$

where $E_{\mathbf{k}}$ is the eigenvalue for the wave number $\mathbf{k}$ within the first Brillouin zone.[14] We have included the first six dominant reciprocal-lattice vectors $\mathbf{K}$ and diagonalized the above equation. The resulting sub-band structure, in energy units of $E_0=\hbar^2K_1^2/m$, is shown in Fig. 1 as function of the wave vector which is in units of $K_1=4\pi/(\sqrt{3}a)$, where a is the lattice constant of the WC. The definition of the high-symmetry points J, X, and Γ in the Brillouin zone are given in Ref. 12. We use the material constants for GaAs: $\epsilon=12.53$ and $m=0.067m_0$ with m_0 the electron mass in vacuum and considered an electron density $n_s=10^{11}$ cm^{-2}. This results in $a=34.0$ nm and gives the units $K_1=2.13\times10^6$ cm^{-2} and $E_0=51.6$ meV. Notice that near the Γ point, the electron energy spectrum is parabolic. The periodic WC potential induces gaps in the spectrum which increase with decreasing z.

Expanding the electron energy around the Γ point, and considering the parabolic dispersion as $E=\hbar^2k^2/2m^*$, allows us to define the effective mass of the remote electron

$$\frac{m^*}{m}=1+24\left(\frac{2\pi n_s}{a_BK_1^3}\right)^2\exp(-2zK_1), \tag{5}$$

where the dominant first six reciprocal-lattice vectors are taken into account in Eq. (4) and $K_1=4\pi/(\sqrt{3}a)$ and $a_B=\hbar\varepsilon/me^2$. Notice that increasing the remote electron separation z from the 2DES suppresses exponentially the static mass enhancement, as one would expect intuitively.

III. WIGNER CRYSTAL PHONONS IN A MAGNETIC FIELD

A. Hamiltonian of a Wigner phonon in a magnetic field

We denote the electron position $\mathbf{r_n}$ in the WC by $\mathbf{r_n}=\mathbf{R_n}+\mathbf{u_n}$, where $\mathbf{R_n}$ are the hexagonal lattice vectors, and $\mathbf{u_n}$ is the displacement of the lattice electron. The Hamiltonian $H_{\rm ph}$ describing the lattice vibrations is now represented in terms of the canonical conjugate momenta: $\mathbf{u_n}$ and $\mathbf{p_n}$. If we assume that the total angular momentum of the electrons vanishes, and introduce the Fourier transforms of $\mathbf{u_n}$ and $\mathbf{p_n}$ given by

$$\mathbf{u_n}=\frac{1}{\sqrt{N}}\sum_{\mathbf{k}}\mathbf{u}(\mathbf{k})\exp(i\mathbf{k}\cdot\mathbf{R}_{\rm n}), \tag{6a}$$

$$\mathbf{p_n}=\frac{1}{\sqrt{N}}\sum_{\mathbf{k}}\mathbf{p}(\mathbf{k})\exp(i\mathbf{k}\cdot\mathbf{R}_{\rm n}), \tag{6b}$$

where N is the total number of electrons, we obtain the Hamiltonian in $\mathbf{k}$ space[13]

$$H_{\rm ph}=\sum_{\mathbf{k}}\left\{\frac{1}{2m}\boldsymbol{\pi}(\mathbf{k})\cdot\boldsymbol{\pi}(-\mathbf{k})+\frac{1}{2}\mathbf{u}(\mathbf{k})\cdot\mathbf{C}(\mathbf{k})\cdot\mathbf{u}(-\mathbf{k})\right\}. \tag{7}$$

The first term is the kinetic energy of the electrons under a uniform magnetic field B applied perpendicular to the WC plane (i.e., xy plane) and the momentum $\boldsymbol{\pi}(\mathbf{k})$ in the symmetric gauge is defined by

$$\boldsymbol{\pi}(\mathbf{k})=\mathbf{p}(\mathbf{k})-\frac{m\omega_c}{2}\overleftrightarrow{\sigma}\cdot\mathbf{u}(-\mathbf{k}), \tag{8}$$

with $\omega_c=eB/mc$ the cyclotron frequency, m the electron mass in the host material, $-e$ the electron charge, c the velocity of light, and $\overleftrightarrow{\sigma}$ the 2D tensor

$$\overleftrightarrow{\sigma}=\begin{pmatrix}0 & 1\\ -1 & 0\end{pmatrix}. \tag{9}$$

The second term in Eq. (7) is the distortion energy of the WC lattice calculated in the harmonic approximation, i.e., up to second order in the displacement $\mathbf{u}$, so that $\overleftrightarrow{C}(\mathbf{k})$ is the elastic tensor defined by

$$\overleftrightarrow{C}(\mathbf{k})=\sum_{\mathbf{n}}\overleftrightarrow{\Phi}(\mathbf{R_n})\{1-\exp(i\mathbf{k}\cdot\mathbf{R_n})\}. \tag{10}$$

Here,

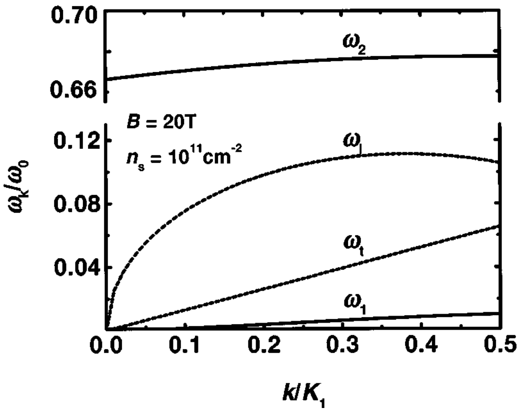

FIG. 2. The frequencies of the WC phonons: ω_l and ω_t are the longitudinal and transverse modes, respectively, in the absence of a magnetic field, and ω_1 and ω_2 are the hybrid modes under a magnetic field of $B=20$ T. The unit of frequency is $\omega_0=E_0/\hbar=7.86\times10^{13}\ \mathrm{s}^{-1}$.

$$\overleftrightarrow{\Phi}(\mathbf{R})_{\alpha\beta}=\frac{1}{2}\left(\frac{\partial^2}{\partial X_\alpha\partial X_\beta}+\frac{\partial^2}{\partial X_\beta\partial X_\alpha}\right)\frac{e^2}{\epsilon|\mathbf{R}|}, \tag{11}$$

is the force tensor, where $|\mathbf{R}|=\sqrt{X_x^2+X_y^2}$ and the subscripts α and β indicate the x or y component. The quantization is performed by introducing the commutation relations between $\mathbf{p}(\mathbf{k})$ and $\mathbf{u}(\mathbf{k})$:

$$[\mathbf{p}(\mathbf{k})_\alpha,\mathbf{u}(\mathbf{k}')_\beta]=-i\hbar\,\delta_{\alpha\beta}\delta_{\mathbf{k}\mathbf{k}'}. \tag{12}$$

B. Diagonalization of the Hamiltonian

In the absence of a magnetic field the diagonalization of the Hamiltonian (7) is discussed by several authors and results into longitudinal and transverse phonon modes.[11,12] According to the most comprehensive study by Bonsall and Maradudin,[12] the Hamiltonian is diagonalized with the transverse and longitudinal conjugate coordinates $Q_l(\mathbf{k})$, $P_l(\mathbf{k})$ and $Q_t(\mathbf{k})$, $P_t(\mathbf{k})$, which are defined by

$$\mathbf{u}(\mathbf{k})=\sum_{\alpha=l,t}Q_\alpha(\mathbf{k})\mathbf{e}_\alpha(\mathbf{k}), \tag{13a}$$

$$\mathbf{p}(\mathbf{k})=\sum_{\alpha=l,t}P_\alpha(\mathbf{k})\mathbf{e}_\alpha(\mathbf{k}), \tag{13b}$$

with

$$\mathbf{e}_\alpha(\mathbf{k})=\begin{cases} i\mathbf{k}/k & (\alpha=l)\\ -i\overleftrightarrow{\sigma}\cdot\mathbf{k}/k & (\alpha=t),\end{cases} \tag{14}$$

where l and t represent the longitudinal and transverse mode, respectively. The eigenvalues $\hbar\omega_\alpha(\mathbf{k})$ ($\alpha=l,t$), or the eigenfrequencies, are given by

$$\omega_l(\mathbf{k})^2=\frac{2\pi e^2 n_s}{\epsilon m}(k-0.181\,483ak^2), \tag{15a}$$

$$\omega_t(\mathbf{k})^2=\frac{2\pi e^2 n_s}{\epsilon m}0.036\,296\,7ak^2, \tag{15b}$$

which are valid up to second order in $k=|\mathbf{k}|$. These frequencies are plotted in Fig. 2.

When a magnetic field is present, the eigenvalues were already obtained in Refs. 12 and 13. We present an alternative derivation of the eigenvalues and eigenvectors by using the fact that the diagonalization is equivalent to solving the equations of motion. Details of the calculation are given in the appendix and we limit ourselves here to the results.

In the presence of a magnetic field the longitudinal and transverse coordinates $Q_\alpha(\mathbf{k})$ ($\alpha=l,t$) perform cyclotron motion which can be separated into two new coordinates

$$Q_\alpha(\mathbf{k})=\sum_{j=1,2}Q_{j\alpha}(\mathbf{k}), \tag{16}$$

where the momentum coordinate (6b) will now also be dependent on these new coordinates (see the appendix). The new coordinate $\Sigma_\alpha Q_{j\alpha}(\mathbf{k})\mathbf{e}_\alpha(\mathbf{k})$, denoted by the index j, is an admixture of longitudinal and transverse motion and in fact exhibits an elliptic motion with eigenfrequency ω_j ($j=1,2$) which is given by

$$\omega_j^2=\frac{1}{2}[(\omega_l^2+\omega_t^2+\omega_c^2)\pm\sqrt{(\omega_l^2+\omega_t^2+\omega_c^2)^2-4\omega_l^2\omega_t^2}], \tag{17}$$

where the $\pm$ sign is chosen such that $\omega_1<\omega_2$. The new four coordinates $Q_{j\alpha}(\mathbf{k})$ ($j=1,2;\alpha=l,t$) satisfy the following commutation relations:

$$[Q_{j\alpha}(\mathbf{k}),Q_{j'\alpha}(\mathbf{k}')]=0, \tag{18a}$$

$$[Q_{jl}(\mathbf{k}),Q_{j't}(\mathbf{k}')]=-i(-1)^j 2d^2(\mathbf{k})\,\delta_{jj'}\delta_{\mathbf{k}\mathbf{k}'}, \tag{18b}$$

with

$$d^2(\mathbf{k})=\frac{\hbar\omega_c}{2m\{\omega_2^2(\mathbf{k})-\omega_1^2(\mathbf{k})\}}. \tag{19}$$

Because two of these four $Q_{j\alpha}(\mathbf{k})$ are independent, we can define new annihilation and creation operators $a_{j\mathbf{k}}$ and $a_{j\mathbf{k}}^\dagger$ such that

$$Q_{jl}(\mathbf{k})=d(\mathbf{k})\mu_j(\mathbf{k})(a_{j\mathbf{k}}+a_{j-\mathbf{k}}^\dagger), \tag{20a}$$

$$Q_{jt}(\mathbf{k})=-i(-1)^j d(\mathbf{k})\mu_j(\mathbf{k})^{-1}(a_{j-\mathbf{k}}-a_{j\mathbf{k}}^\dagger), \tag{20b}$$

where

$$\mu_j(\mathbf{k})=\left\{\frac{|\omega_t^2(\mathbf{k})-\omega_j^2(\mathbf{k})|}{\omega_c\omega_j(\mathbf{k})}\right\}^{1/2}. \tag{21}$$

Then, the commutation relations (18a) and (18b) become

$$[a_{j\mathbf{k}},a_{j'\mathbf{k}'}^\dagger]=\delta_{jj'}\delta_{\mathbf{k}\mathbf{k}'},\quad (j,j'=1,2). \tag{22}$$

With these creation and annihilation operators the Hamiltonian (7) is now diagonalized and takes the form

$$H_{\mathrm{ph}}=\sum_{\mathbf{k}}\sum_{j=1,2}\hbar\omega_j(\mathbf{k})\left(a_{j\mathbf{k}}^\dagger a_{j\mathbf{k}}+\frac{1}{2}\right). \tag{23}$$

In Fig. 2, the $\mathbf{k}$ dependence of ω_j is shown for $n_s=10^{11}\ \mathrm{cm}^{-2}$ at $B=20$ T. In the zero magnetic field limit the frequency $\omega_2(\mathbf{k})$ converges to the longitudinal frequency $\omega_l(\mathbf{k})$ which couples strongly with the remote electron.

However, in large magnetic fields this phonon has a large energy and is therefore difficult to excite. The remote electron will mainly couple to the low-energy excitation $\omega_1(\mathbf{k})$, which converges to $\omega_t(\mathbf{k})$. In fact, in the absence of a magnetic field this frequency mode does not interact with the remote electron.

IV. REMOTE WIGNER POLARON

A. Electron-phonon interaction

We consider the deformation of the lattice due to the presence of a remote electron a distance z away from the WC. Such an electron locally polarizes the WC which can be viewed as the excitation of virtual phonons of the WC. Taking into account the Coulomb potential between the remote electron at $(\mathbf{r},z)$ and the lattice electrons at $\mathbf{R_n}$, we obtain the interaction energy as

$$H_{\rm int}=\frac{e^2}{\epsilon}\sum_{\mathbf{n}}\left\{\frac{1}{\sqrt{[\mathbf{r}-\mathbf{R_n}-\mathbf{u}(\mathbf{R_n})]^2+z^2}}-\frac{1}{\sqrt{(\mathbf{r}-\mathbf{R_n})^2+z^2}}\right\}. \tag{24}$$

Next, we consider only small deviations from the equilibrium lattice positions and linearize $H_{\rm int}$ in the variable $\mathbf{u}(\mathbf{R_n})$ which, with use of Eq. (6a) and the 2D ϑ function relation,[15] results in the expression

$$H_{\rm int}=\frac{-i2\pi e^2 n_s}{\epsilon\sqrt{N}}\sum_{\mathbf{k}}\mathbf{u}(\mathbf{k})\cdot\sum_{\mathbf{K}}\frac{\mathbf{k}+\mathbf{K}}{|\mathbf{k}+\mathbf{K}|}\times\exp[-z|\mathbf{k}+\mathbf{K}|+i(\mathbf{k}+\mathbf{K})\cdot\mathbf{r}]. \tag{25}$$

If we consider the long-wavelength limit, and ignore Umklapp processes by dropping the sum over the reciprocal-lattice vectors $\mathbf{K}$ and keeping only the $\mathbf{K}=0$ term, the electron will only interact with the longitudinal phonons. Using the relations (13a), (16), (20a), and (20b), we obtain the second-quantized expression of the Hamiltonian as

$$H_{\rm int}=\sum_{\mathbf{k}}\sum_{j=1,2}\frac{V_{j\mathbf{k}}}{\Omega}\exp(i\mathbf{k}\cdot\mathbf{r})(a_{j\mathbf{k}}+a^\dagger_{j-\mathbf{k}}), \tag{26}$$

where $\Omega(=N/n_s)$ is the system area and the coupling strength $V_{j\mathbf{k}}$ is $\mathbf{k}$ and z dependent and given by

$$V_{j\mathbf{k}}=\frac{2\pi e^2 n_s^{1/2}}{\epsilon}d(\mathbf{k})\mu_j(\mathbf{k})\exp(-kz). \tag{27}$$

B. Polaron in a magnetic field

The full Hamiltonian H for the Wigner polaron interacting with the Wigner crystal phonons in a magnetic field is then given by

$$H=\frac{1}{2m^*}\left(\mathbf{p}+\frac{e}{c}\mathbf{A}(\mathbf{r})\right)^2+H_{\rm ph}+H_{\rm int}. \tag{28}$$

Here, m^* is the effective mass of the remote electron in the static WC defined by Eq. (5), $\mathbf{A}(\mathbf{r})=\mathbf{B}\times\mathbf{r}/2$ is the symmetric gauge vector potential, $H_{\rm ph}$ is the WC phonon Hamiltonian (7) and $H_{\rm int}$ is the interaction Hamiltonian given by Eq. (24).

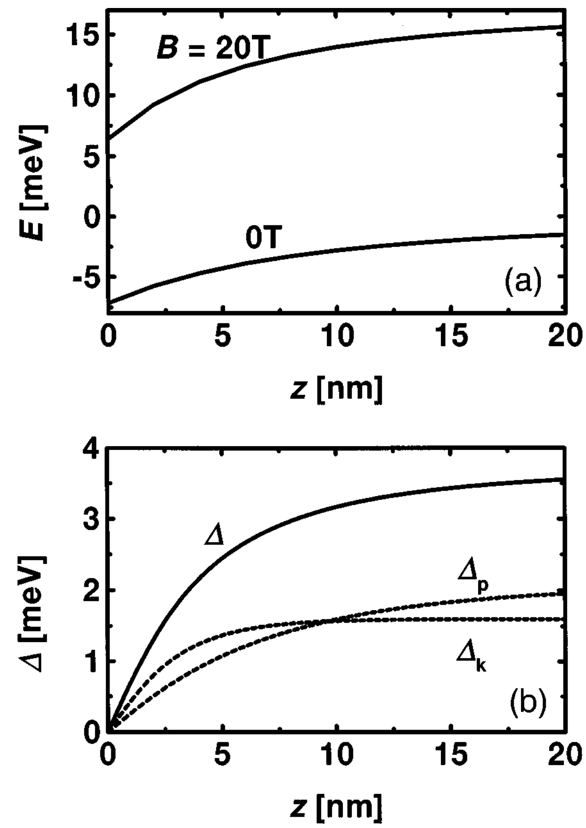

FIG. 3. The z dependence of E: the polaron energy correction caused by the interaction of the remote electron with the WC phonons and the magnetic field for $B=0$ and 20 T (a), and the energy shift Δ caused by the magnetic field (b). The electron density is taken to be $n_s=10^{11}$ cm^{-2}.

Using second-order perturbation theory, we obtain the ground-state energy E of the coupled system as[16]

$$E=\frac{1}{2}\hbar\omega_c^*+\delta E, \tag{29}$$

where ω_c^* is the cyclotron frequency defined by $\omega_c^*=eB/m^*c$ and δE is the energy correction[17] caused by the WC phonons,

$$\delta E=-\frac{1}{\Omega}\sum_{\mathbf{k}}\sum_{j=1,2}\frac{|V_{j\mathbf{k}}|^2}{\hbar\omega_j(\mathbf{k})}\int_0^\infty d\tau\exp\left[-\tau+k^2D_{\rm B}\left(\frac{\tau\omega_c^*}{\omega_j(\mathbf{k})}\right)\right], \tag{30}$$

with

$$D_{\rm B}(\xi)=\frac{\hbar}{2m^*\omega_c^*}[1-\exp(-\xi)]. \tag{31}$$

Here, we have shifted the energy E by the zero-point energy of the phonons.

In Fig. 3(a), the z dependence of the remote electron energy E is shown for $B=0$ and 20 T by the solid curves when $n_s=10^{11}$ cm^{-2}. An electron out of the WC plane feels an attractive force (in addition to the electrostatic repulsive force due to the static WC) caused by the polarization due to the electron-WC interaction. To move an electron from the WC plane at $z=0$ to the remote position z, the following correlation energy $W(z,B)=E(z,B)-E(0,B)$ is needed,

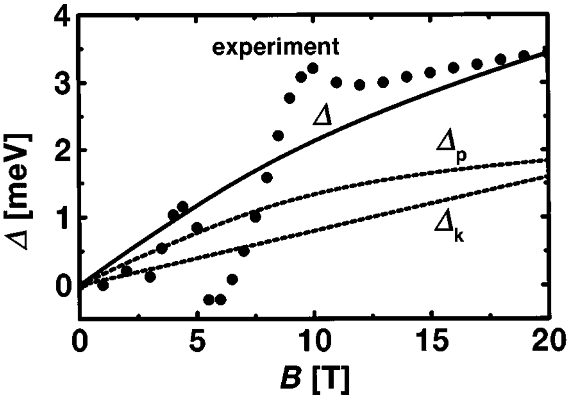

FIG. 4. The energy shift Δ and its components Δ_p and Δ_k as function of the magnetic field. The dots are the experimental results of Lok *et al.* We took $n_s = 10^{11}$ cm^{-2} and $z = 15$ nm.

which increases with increasing field strength B. This is due to the fact that the phonon frequency ω_1 decreases with B. This correlation energy is very likely related to the Coulomb (quasi) gaps seen in a resonant experiment when a single electron tunnels into the WC (Ref. 18) or biased emitter.[19,9] When a tunneling electron moves from the WC plane at $z = 0$ to the quantum well located at z, the electron loses an energy $W(z,B)$, which has to be supplied to the system, and this is equivalent to having to apply a higher bias field. Consequently, this results in a shift of the tunneling resonance position. Recently, a shift Δ in the position of the resonant peak at high magnetic fields was observed.[9] Within our model this shift is given by $\Delta(z,B) = W(z,B) - W(z,0)$. In Fig. 3(b) the energy shift Δ is shown as a function of z for $B = 20$ T. This energy shift is composed of a phonon part $\Delta_p = W_p(z,B) - W_p(0,B)$ and a kinetic part $\Delta_k = W_k(z,B) - W_k(0,B)$, which are shown by the dashed curves.

Since in the experiment of Ref. 9 there is some ambiguity about the values of n_s and z, one cannot carry out a strict comparison with our calculations. However, the experimentally observed shift is about 3 meV for $n_s \simeq 10^{11}$ cm^{-2} at $B = 20$ T, which is comparable in size to our $\Delta(z,B)$. In a previous paper, we calculated the energy shift Δ under the assumption that the remote electron couples with the plasmon excitations of the 2D electron gas.[10] This explained the experimentally observed oscillations in Δ with B, but there was still a factor of 4 difference between the measured and calculated values. In this paper, this difference is improved in the high magnetic field regime. This is due to the inclusion of the mass enhancement of the remote electron as a consequence of the static periodic potential of the WC,[8] and the interaction with the hybrid phonon mode with frequency ω_1. The improvement is mainly achieved by the hybrid phonon mode whose frequency ω_1 is smaller than the plasmon mode and causes a large shift of the polaron energy.

In Fig. 4 the B dependence of the energy shift $\Delta(z,B)$ is shown. Notice that under the assumption of reasonable values for the electron density ($n_s = 10^{11}$ cm^{-2}) and the distance between the remote electron and the 2DES ($z = 15$ nm we found quantitative agreement (in magnitude and in the functional behavior of Δ with B) with the experimental results of Lok *et al.*[9] in the high magnetic-field region, i.e., $B > 10$ T where the 2DES is expected to be strongly correlated and near the WC phase. Although it is clear that in a strict sense the WC is not formed at low magnetic fields, this description takes into account that the electrons in the 2DES are strongly correlated and form locally an imperfect crystallike configuration. The experimental data of Ref. 9 exhibit an oscillatory behavior with B, which is not apparent in Fig. 4. This oscillation is related to the occupation of Landau levels which influences the electron-electron screening and in turn the remote electron-WC correlation and was explained in Ref. 10. The latter plasmon-type of approach is more applicable in the low magnetic-field region, i.e., $B < 10$ T. It underestimated the electron-electron correlation in the 2DES in the high magnetic-field region.

V. CONCLUSIONS

The 2DES in the presence of a strong perpendicular magnetic field forms a WC. A remote electron a distance away from the 2DES will be repelled due to the static lattice, but it will feel an attractive contribution due to the polarization of the WC. We formulated the remote electron problem as a *Wigner polaron* problem in a magnetic field and used second-order perturbation theory to calculate this attractive potential. We also took into account the mass enhancement caused by the periodic potential of the static WC. In the absence of a magnetic field the WC has longitudinal and transverse phonons and the remote electron interacts predominantly with the longitudinal mode. In the presence of a magnetic field, on the other hand, these two modes are hybridized and result in two new modes. We obtained the coordinates of these hybrid phonons by solving the equations of motion in the Heisenberg picture.

The attractive potential between the remote electron and the WC is related to an energy shift obtained experimentally in a resonant tunneling experiment. The energy shift at high magnetic fields is explained by the difference of the attractive potential at zero and nonzero magnetic field. The agreement between the measured and the theoretical energy shifts[10] is improved by the inclusion of the hybrid phonon modes due to the magnetic field and the mass enhancement caused by the periodic potential of the WC. Agreement with experiment is found in the high magnetic-field regime, i.e., $B > 10$ T, where the present model is expected to be applicable.

ACKNOWLEDGMENTS

One of the authors (H.K.) is supported by a grant from the Japanese Ministry of Education, Culture and Science, and F.M.P. is partially supported by the Flemish Science Foundation (FWO). We thank A. Geim, G. Goldoni, I. Lok, and I. Marmorkos for discussions. We would also like to thank S. Ulloa for a critical reading of the manuscript and for stimulating discussions. Part of this work is supported by the FWO and a NATO collaborative research grant.

APPENDIX: DIAGONALIZATION OF THE WIGNER-PHONON HAMILTONIAN

In this appendix, the Hamiltonian (7) is diagonalized by solving the equations of motion in the Heisenberg picture.

As explained in Sec. III, we introduce new coordinates $\mathbf{Q}(\mathbf{k})=(Q_l(\mathbf{k}),Q_t(\mathbf{k}))$ and $\mathbf{P}(\mathbf{k})=(P_l(\mathbf{k}),P_t(\mathbf{k}))$ defined by Eqs. (13a) and (13b). Then, the commutation relations (12) transform into

$$[\mathbf{P}(\mathbf{k})_\alpha,\mathbf{Q}(\mathbf{k}')_\beta]=-i\hbar\,\delta_{\alpha\beta}\delta_{\mathbf{kk}'},\quad(\alpha,\beta=l,t)\tag{A1}$$

and the equations of motion in the Heisenberg picture become

$$\frac{\mathrm{d}}{\mathrm{d}t}\mathbf{Q}(t)=\frac{1}{m}\mathbf{P}(t),\tag{A2a}$$

$$\frac{\mathrm{d}}{\mathrm{d}t}\mathbf{\Pi}(t)=-\omega_c\overleftrightarrow{\sigma}\cdot\mathbf{\Pi}(t)+\overleftrightarrow{C}'\cdot\mathbf{Q}(t),\tag{A2b}$$

where t is the time and the $\mathbf{k}$ dependence is not indicated explicitly. The momentum $\mathbf{\Pi}(t)$ and associated $\overleftrightarrow{C}'$ tensor are defined by

$$\mathbf{\Pi}(t)=\mathbf{P}(t)-m\omega_c^2\overleftrightarrow{\sigma}\cdot\mathbf{Q}(t),\tag{A3}$$

$$\overleftrightarrow{C}'=\begin{pmatrix}m\omega_l^2 & 0\\ 0 & m\omega_t^2\end{pmatrix}.\tag{A4}$$

Because the differential Eqs. (A2a) and (A2b) are linear, a Laplace transformation reduces them to algebraic equations. We denote $\tilde{\mathbf{Q}}(s)$ as the Laplace transform of $\mathbf{Q}(t)$. Applying the formula $\widetilde{df/dt}(s)=s\tilde{f}(s)-f(0)$ to Eqs. (A2a) and (A2b), we obtain

$$\tilde{\mathbf{Q}}(s)=\frac{1}{D(s)}\begin{pmatrix}s^2+\omega_l^2 & -s\omega_c\\ s\omega_c & s^2+\omega_t^2\end{pmatrix}\left\{\begin{pmatrix}s & \omega_c\\ -\omega_c & s\end{pmatrix}\cdot\mathbf{Q}+\frac{\mathbf{\Pi}}{m}\right\},\tag{A5}$$

where $\mathbf{Q}=\mathbf{Q}(0)$, $\mathbf{\Pi}=\mathbf{\Pi}(0)$, and

$$D(s)=(s^2+\omega_l^2)(s^2+\omega_t^2)+s^2\omega_c^2.\tag{A6}$$

The zero points of $D(s)$ are denoted by $s=\pm i\omega_j$ $(j=1,2)$, where ω_j is the eigenfrequency of the new modes given by Eq. (17).

The inverse Laplace transform now leads to

$$\mathbf{Q}(t)=\sum_{j=1,2}[\mathrm{Res}_{s=i\omega_j}\tilde{\mathbf{Q}}(s)\exp(-st)+\mathrm{Res}_{s=-i\omega_j}\tilde{\mathbf{Q}}(s)\exp(-st)],\tag{A7}$$

where Res denotes the residue. The resulting expression is

$$\mathbf{Q}(t)=\sum_{j=1,2}\overleftrightarrow{\Omega}_j(t)\cdot\mathbf{Q}_j,\tag{A8}$$

where

$$\mathbf{Q}_j=\frac{-(-1)^j}{(\omega_2^2-\omega_1^2)\omega_j^2}\left\{\left(\omega_l^2\omega_t^2-\omega_j^2\frac{\overleftrightarrow{C}'}{m}\right)\cdot\mathbf{Q}+\omega_j^2\omega_c^2\overleftrightarrow{\sigma}\cdot\mathbf{\Pi}\right\},\tag{A9}$$

and $\overleftrightarrow{\Omega}_j(t)$ is a tensor which elliptically rotates the coordinate $\mathbf{Q}_j$ and is defined by

$$\overleftrightarrow{\Omega}_j(t)=\cos\omega_jt+\overleftrightarrow{\sigma}\cdot\frac{1}{\omega_j\omega_c}\left(\frac{\overleftrightarrow{C}'}{m}-\omega_j^2\right)\sin\omega_jt.\tag{A10}$$

With the same treatment for $\mathbf{\Pi}(t)$, we obtain

$$\mathbf{\Pi}(t)=\sum_{j=1,2}\overleftrightarrow{\Omega}_j(t)\cdot\mathbf{\Pi}_j,\tag{A11}$$

where

$$\mathbf{\Pi}_j=\frac{m}{\omega_c}\overleftrightarrow{\sigma}\cdot\left(\frac{\overleftrightarrow{C}'}{m}-\omega_j^2\right)\cdot\mathbf{Q}_j.\tag{A12}$$

With the new coordinates the Hamiltonian (7) becomes

$$H_{\mathrm{ph}}=\sum_{\mathbf{k}}\sum_{j=1,2}\frac{\hbar\omega_c\omega_j(\mathbf{k})^2}{d(\mathbf{k})^2}\left\{\frac{Q_{jl}(\mathbf{k})Q_{jl}(-\mathbf{k})}{|\omega_t(\mathbf{k})^2-\omega_j(\mathbf{k})^2|}+\frac{Q_{jt}(\mathbf{k})Q_{jt}(-\mathbf{k})}{|\omega_l(\mathbf{k})^2-\omega_j(\mathbf{k})^2|}\right\}.\tag{A13}$$

The commutation relations (18a) and (18b) are derived from the definition (A9) and the factor $\mu_j(\mathbf{k})$ in Eqs. (20a) and (20b) originates from the term of $Q_{j\alpha}(\mathbf{k})Q_{j\alpha}(-\mathbf{k})$ in Eq. (A13). The Hamiltonian (23) is derived easily from Eqs. (20a), (20b), and (A13).

---

*Permanent address: Hakodate National College of Technology, 14-1 Tokura-cho Hakodate, 042 Hokkaido, Japan. Electronic address: kato@cc.hakodate-ct.ac.jp

†Electronic address: peeters@uia.ua.ac.be

[1] F. M. Peeters, in *The Two-Dimensional Electron Systems on Helium and other Cryogenic Substrates*, edited by E. Y. Andrei (Kluwer Academic Publishers, Dordrecht, 1997), p. 17.

[2] *Low-Dimensional Electronic Systems*, edited by G. Bauer, F. Kuchar, and H. Heinrich (Springer-Verlag, Berlin, 1992).

[3] C. C. Grimes and G. Adams, Phys. Rev. Lett. **42**, 795 (1979); D. C. Glattli, E. Y. Andrei, and F. I. B. Williams, *ibid.* **60**, 420 (1988); M. A. Stan and A. J. Dahm, Phys. Rev. B **40**, 8995 (1989).

[4] E. Y. Andrei, G. Deville, D. C. Glattli, F. I. B. Williams, E. Paris, and B. Etienne, Phys. Rev. Lett. **60**, 2765 (1988).

[5] G. S. Boebinger, H. W. Jiang, L. N. Pfeiffer, and K. W. West, Phys. Rev. Lett. **64**, 1793 (1990).

[6] Y. W. Suen, L. W. Engel, M. B. Santos, M. Shayegan, and D. C. Tsui, Phys. Rev. Lett. **68**, 1379 (1992).

[7] L. Zheng and H. A. Fertig, Phys. Rev. B **52**, 12 282 (1995); S. Narasimhan and T. L. Ho, *ibid.* **52**, 12 291 (1995); G. Goldoni and F. M. Peeters, *ibid.* **53**, 4591 (1996); Europhys. Lett. **37**, 293 (1997); *ibid.* **38**, 319 (1997).

[8] H. Kato, F. M. Peeters, and S. E. Ulloa, Europhys. Lett. **40**, 551 (1997).

[9] J. G. S. Lok, A. K. Geim, J. C. Maan, L. Eaves, A. Nogaret, P. C. Main, and M. Henini, in *Proceedings of the 23rd International Conference on the Physics of Semiconductors*, edited by M. Scheffler and R. Zimmerman (World Scientific, Singapore, 1996), p. 2315; Phys. Rev. B **56**, 1053 (1997).

[10] H. Kato, F. M. Peeters, and S. E. Ulloa, Europhys. Lett. **45**, 235 (1999).

[11] R. S. Crandall, Phys. Rev. A **8**, 2136 (1973); P. M. Platzmann and H. Fukuyama, Phys. Rev. B **10**, 3150 (1974).

[12] L. Bonsall and A. A. Maradudin, Phys. Rev. B **15**, 1959 (1977).

[13] H. Fukuyama, Solid State Commun. **17**, 1323 (1975); V. I. Falko, Phys. Rev. B **49**, 7774 (1994).

[14] C. Kittel, *Introduction to Solid State Physics* (John Wiley & Sons Inc., New York, 1971).

[15] J. M. Ziman, *Principles of the Theory of Solids* (Cambridge University Press, Cambridge, 1972).

[16] S. Das Sarma, Phys. Rev. Lett. **52**, 859 (1984); F. M. Peeters and J. T. Devreese, Phys. Rev. B **31**, 3689 (1985); D. M. Larsen, *ibid.* **33**, 799 (1986).

[17] X. G. Wu, F. M. Peeters, and J. T. Devreese, Phys. Rev. B **32**, 7964 (1985).

[18] J. P. Eisenstein, L. N. Pfeiffer, and K. W. West, Phys. Rev. Lett. **69**, 3804 (1992); K. M. Brown, N. Turner, J. T. Nicholls, E. H. Linfield, M. Pepper, D. A. Ritchie, and G. A. C. Jones, Phys. Rev. B **50**, 15 465 (1994).

[19] G. S. Boebinger, A. F. J. Levi, A. Passner, L. N. Pfeiffer, and K. W. West, Phys. Rev. B **47**, 16 608 (1993).